Telis, VRN.; Martínez Navarrete, N. (2010). Application of compression test in analysis of mechanical and color changes in grapefruit juice powder as related to glass transition and water activity. Food Science and Technology. 43(5):744-751. doi:10.1016/j.lwt.2009.12.007.

APPLICATION OF COMPRESSION TEST IN ANALYSIS OF MECHANICAL AND COLOR CHANGES IN GRAPEFRUIT JUICE POWDER AS RELATED TO GLASS TRANSITION AND WATER ACTIVITY

Telis, V.R.N.[2], Martínez-Navarrete, N.[1,*]

[1]UPV – Universidad Politécnica de Valencia, Departamento de Tecnología de Alimentos, Camino de Vera 14, 46022 Valencia, Spain.

[2]UNESP – Universidade Estadual Paulista, Departamento de Engenharia e Tecnologia de Alimentos, 15054-000 São José do Rio Preto, São Paulo, Brazil.

*Corresponding author: Tel.: +34-963879362, Fax: +34-963877369

E-mail address: nmartin@tal.upv.es

Running Head – Mechanical and color changes in grapefruit powder…

Abstract

Physicochemical and structural properties of grapefruit juice powder were studied as affected by water activity. Powdered juice was obtained by freeze-drying and equilibrated at different water vapor pressure atmospheres in order to give samples with water activity in the range of 0 to 0.84. The mechanical properties of the powder were measured by confined compression tests and the compressed samples, which presented uniform surface and thickness, were subjected to color analysis. The maximum force attained during the compression tests and the color

coordinates could be quantified with good reproducibility. The results were related to water activity and to glass transition temperature. The occurrence of mechanical changes in the powder was shown to precede significant color changes with increasing water activity. Considering the susceptibility to stickiness, the stability limit was observed at $T - T_g \approx 2$ ºC, with a high degree of mechanical changes being detected at $T - T_g \approx 16$ ºC, whereas for significant color changes this critical temperature difference was around 32 ºC.

Key Words: Water Content, Sorption Isotherm, Stickiness, Freeze-drying

Nomenclature

A	parameter in Equation (4)
a*	CIELab color coordinate
a_w	water activity
a_{whalf}	parameter in Equation (7)
b*	CIELab color coordinate
C_{ab}*	chroma
F_l	parameter in Equation (7), N/kg
F_{max}	maximum force attained during the compression test, N
F_u	parameter in Equation (7), N/kg
h_{ab}*	hue angle, degrees
k	parameter in Equation (5)
L*	CIELab color coordinate
m	sample mass, kg
T	temperature, ^oC

T_{gs} glass transition of the anhydrous solids fraction, ^{o}C

T_{gw} glass transition of pure amorphous water (-135 ^{o}C)

X water content, dry basis

X_m monolayer water content, dry basis

X_s solids fraction

X_w water fraction

ΔE^* total color difference

λ parameter in Equation (7)

1. Introduction

Natural fruit juices, and particularly citrus juices, are considered nutrient dense beverages, as they are concentrated sources of nutrients (Rampersaud, 2007). Powdered juices might constitute good alternatives to convenient and healthy food products or ingredients to formulated foods. Nevertheless, drying and storage of powdered fruit juices presents technical difficulties due to their hygroscopic and thermoplastic behavior at high temperature and/or humidity, a characteristic that is associated to their composition (Adhikari, Howes, Bhandari & Troung, 2004). Most of the soluble solids in fruit juices are low molecular weight sugars such as sucrose, glucose and fructose, as well as organic acids such as citric, malic and tartaric acid. Rapid water removal during freeze-drying or spray-drying, which are the methods usually employed in producing powdered fruit juices, results in an amorphous matrix that is susceptible to glass transition related changes, including stickiness, caking, and collapse (Aguilera, Del Valle & Karel, 1995; Chen, 2007; Foster, Bronlund & Paterson., 2006; Phanindrakumar, Radhakrishna, Mahesh, Jagannath & Bawa, 2005; Venir, Munari, Tonizzo & Maltini, 2007), as well as color changes (Acevedo,

Schebor & Buera, 2006; Lievonen, Laaksonen & Roos, 2002; Ling, Birch & Lim, 2005; Miao & Roos, 2006).

The glass transition is characterized by the change from the glassy to the rubbery state, with a certain characteristic of a thermodynamic second-order phase transition over a temperature range. This temperature range is characteristic for each material and may extend over 10 to 20 ºC for amorphous sugars, or up to over 50 ºC for some food polymers. The glass transition temperature (T_g) is taken as the onset or mid-point temperature of such a range and it is usually plasticized by water. When amorphous food materials reach their glass transition temperature, by increasing temperature and/or increasing water content, various time dependent structural transformations may occur as a consequence of the drastic decrease in the viscosity and increase in molecular mobility above T_g (Levine & Slade, 1989; Roos & Karel, 1991; Roos, 1995a, 2003; Slade & Levine, 1991). The highly porous materials prepared by freeze-drying are susceptible to post-drying collapse, characterized by a loss of structure and, in particular, a drastic decrease in porosity, affecting aroma retention, caking and stickiness, rehydration capacity and final moisture distribution (Levi & Karel, 1995). There is a strong dependence of rates of collapse on the quantity ($T - T_g$), and the effect of water is mainly associated with the depression of T_g that leads to the increase in ($T - T_g$) at constant temperature (Aguilera et al. 1995; Fitzpatrick, Hodnett, Twomey, Cerqueira, O'Flynn & Roos, 2007; Foster et al., 2006; Paterson, Brooks, Bronlund & Foster, 2005). According to Roos (1995b), stickiness, caking and collapse, appear to be related phenomena. When a freeze-dried matrix reaches a critical temperature, which is related to T_g, a sequence of deleterious events is observed. Initially, an incipient liquid state of a lower viscosity at the particle surface occurs, which results in stickiness. Caking of sticky powders results because

of interparticle bridging, causing a loss of structure and decrease in sample volume. Collapse may be considered as an extended caking phenomenon that results in liquefaction, reducing the macroscopic volume towards that typical of the liquid state and concomitant loss of porosity.

The methods used to detect collapse and shrinkage ranged from visual observation (To & Flink, 1978) and measurements of specific volume (Venir et al., 2007; Prado, Buera & Elizalde, 2006; Levi & Karel, 1995) to measurements of internal porosity (White & Bell, 1999). Techniques and instrumentations developed for quantifying the degree of stickiness, caking and agglomeration in food powders have been reviewed by Boonyai, Bhandari and Howes (2004), who concluded that efforts on developing an accurate, simpler, and cheaper technique to characterize the stickiness behavior of food powders are still needed.

Boonyai, Howes and Bhandari (2007) developed a thermal compression test that involves the application of compression force in a thermally controlled sample cell attached to a texture analyzer as a method to investigate the glass–rubber transition of food powders. The technique was validated against standard DSC and TMA methods. Özkan, Walisinghe and Chen (2002) applied a penetration test based on the measurement of force required to penetrate powder compacts to characterize stickiness and cake formation in whole and skim milk powders. Compression tests were also used by Al Mahdi, Nasirpour, Banon, Scher and Desobry (2006) to quantify caking intensity of dried skimmed milk and wheat flour, expressed as the maximum force calculated from force/compression curves.

Krokida, Maroulis and Saravacos (2001) pointed out that when compared to other drying methods, freeze-drying seemed to prevent color changes in foods, resulting in dried products with improved color characteristics. Nevertheless, storage

of freeze-dried foods above their glass transition temperature induces reactions of color deterioration such as enzymatic and non-enzymatic browning (Karmas, Buera and Karel, 1992); Miao and Roos, 2006). According to Acevedo et al. (2006), the dependence of browning rate with relative humidity of freeze-dried systems of different compositions and structures was governed by solid–water interactions and by structural characteristics of the systems. Rates of non-enzymatic browning of solid food models were shown to increase at temperatures 10-20 °C above the T_g (Lievonen et al., 2002).

Color measurement in bulk powder presents some drawbacks. Instrument manufacturers point out that when measuring powder color with a spectrophotometer, the measurement value varies depending on the density of the powder and the surface conditions. To avoid errors, special methods are required such as placing a fixed amount of powder into a container of a fixed shape and size and maintaining a fixed surface quality (Konica Minolta Sensing, Inc., 2003). Stickiness and collapse undergone by amorphous food powders during exposure to high water vapor pressure atmospheres may affect color measurement, confounding the effects of browning reactions themselves and of the structural changes suffered by the powder.

The objective of the present work was to evaluate the viability of using mechanical compression as a simple and convenient empirical method for characterizing freeze-dried pink grapefruit juice in terms of stickiness development and color changes as affected by glass transition and water content.

2. Materials and Methods

151 *2.1. Material and sample preparation*

152 Grapefruit (*Citrus paradisi*) of the pigmented variety Star Ruby was obtained
153 in the local market (Valencia, Spain). Fruits were washed and peeled with careful
154 removal of the albedo. The pulp was cut and triturated in a bench top electrical food
155 processor (Thermomix TM 21, Vorwerk, Spain) and passed through a coarse sieve
156 (which is an accessory of the Thermomix) in order to remove most of the fruit rag.
157 This procedure resulted in about 800 mL of juice with the following characteristics:
158 9.20 ± 0.01 ^{o}Brix, measured in an Abbe refractometer (model 3T, Atago, Japan);
159 9.74 ± 0.02 g total solids/100 g total mass determined by the gravimetric method in
160 vacuum oven at 60 ^{o}C to constant weight; water activity (a_w) of 0.985 ± 0.003
161 measured in a water activity meter (model FA-st lab 1, GBX, France); pH of 3.06 ±
162 0.03 measured using a pH meter (model SevenEasy Conductivity, Mettler-Toledo,
163 Switzerland); titratable acidity of 1.74 ± 0.01 g citric acid/100 g total mass,
164 determined by titration to pH 8.2 with NaOH 0.1 mol equi/L.

165 Assuming that the main soluble solids of grapefruit var. Star Ruby are sugars
166 and citric acid (Peiró-Mena, 2007) and taking into account the analyzed amount of
167 total solids and citric acid, the sugars content of the sample used for the study will be
168 around 7.4 g/100 g total mass. Moreover, as pointed out by Peiró-Mena (2007), the
169 main sugars of grapefruit var. Star Ruby are sucrose:fructose:glucose in mass ratio of
170 54:25:21.

171 The juice was rapidly frozen at -25 ^{o}C in thin layers for 48 h before freeze-
172 drying in a Telstar Lioalfa-6 Lyophyliser at 10^{-2} Pa for 24 h. The dry product was
173 ground in a mortar and resulted in a powder with water content of 3.24 ± 0.01 g
174 water/100 g total mass, determined by the gravimetric method, in a vacuum oven at
175 60 ^{o}C, to constant weight. Samples of about 0.6 g of the grapefruit juice powder

spread over watch glasses of 50 mm in diameter, always in triplicate, were conditioned inside vacuum desiccators at 23 ºC. P_2O_5 and saturated salt solutions (LiCl, CH_3COOK, $MgCl_2$, K_2CO_3, $Mg(NO_3)_2$, $NaNO_2$, NaCl, KCl) were used to maintain the water activity (a_w) between 0 and 0.84, according to a static sorption isotherm methodology (Spiess & Wolf, 1983). The sample weights were measured until a constant value was attained, where the equilibrium was assumed to be reached.

2.2. Measurement of T_g

Duplicate samples of about 6 mg, placed directly in DSC sample pans ((P/N SSC000C008, Seiko Instruments, Inc., Japan), were also conditioned in the same relative humidity chambers for glass transition measurement. After equilibration, pans were rapidly weighed and sealed. Calorimetric analysis was carried out using a DSC 220CU-SSC5200 (Seiko instruments, Inc., Japan). Heating rate was 5 ^oC/min and temperature range varied between -100 and 100 ^oC, depending on sample water content. The reference was an empty pan and liquid nitrogen was used for sample cooling before the runs. The midpoint of the glass transition was considered as the characteristic T_g.

2.3. Compression tests and color measurement

Mechanical compression tests were conducted using a texture analyzer TA-XT Plus (Stable Micro Systems, Ltd., UK), using a cylindrical probe of 10 mm diameter. Samples of juice powder conditioned at the different a_w were placed in a circular aluminum sample holder of 11 mm diameter and 5.5 mm height. The bottom of the sample holder was hollowed and a sliding white polyethylene disc of 10 mm in

diameter and 1 mm thickness was used to close the bottom (Figure 1). During compression tests, the sample holder was kept in a fixed position by fitting in a cavity of diameter only slightly greater than the holder, made in a plate that served as the basis for the compression test. The sample holder was filled up with sample and placed on the plate cavity. The sample was then compressed for a fixed distance of 3 mm at a constant rate of 0.05 mm/s. The maximum force attained during the test was recorded as F_{max}.

The sample holder containing the compressed sample was then rapidly inverted over a small reflectance glass (CR-A51, Minolta Camera Co., Japan) which was fixed upon the spectrophotomer lens (mod. CM-2002, Minolta Camera Co., Japan), providing a measurement window of 6 mm diameter. Finally, the sample was forced against the glass surface by pushing the sliding polyethylene disc in the bottom of the sample holder, thus providing a uniform surface and thickness for assaying color by measuring the CIELab color coordinates with a D65 illuminant and 10^o observer. In this system the coordinate L* denotes lightness on a 0 to 100 scale from black to white; a*, (+) red or (-) green; and b*, (+) yellow or (-) blue. The hue angle (h_{ab}*), chroma (C_{ab}*), and total color differences (ΔE*) with respect to samples conditioned over P_2O_5 were also obtained as given by Equations (1), (2) and (3) (Fernandez-Segovia, Camacho, Martinez-Navarrete, Escriche & Chiralt, 2003).

$$\Delta E^* = \sqrt{(\Delta L^*)^2 + (\Delta a^*)^2 + (\Delta b^*)^2} \quad (1)$$

$$C_{ab}{}^* = \sqrt{(a^*)^2 + (b^*)^2} \quad (2)$$

$$h_{ab}{}^* = \text{arctg}\left(\frac{b^*}{a^*}\right) \quad (3)$$

After color measurement, when the sample was still over the glass, the sample holder was carefully removed and the sample thickness was determined with a digital

225 caliper.

226

227 **3. Results and Discussion**

228

229 *3.1. Sorption behavior*

230 The experimental results of the equilibrium water content at 23 ^{o}C and nine
231 levels of water activity are presented in Figure 2. Each point is the average of three
232 determinations. An unusual behavior in the experimental data was observed in
233 samples conditioned over P_2O_5, which presented a small amount of residual water
234 content (about 0.02 kg water/kg dry matter). Bonelli, Schebor, Cukierman, Buera and
235 Chirife (1997) and Brooks, Paterson and Bronlund (2001) have already reported the
236 presence of residual water in samples of freeze-dried sugar matrices desiccated over
237 P_2O_5 at room temperature.

238 The Caurie model (Caurie, 1970; Vega-Gálvez, Lemus-Mondaca, Fito and
239 Andrés, 2007), given by Equation (4), was used for adjusting the experimental data
240 of equilibrium water content versus a_w, according to the curve showed in Figure 2.
241 The selection of Caurie´s equation may be justified taking into account its ability of
242 predicting some residual moisture in the product at zero water activity.

243 $$X = \exp\left[a_w \ln(A) - \frac{1}{4.5X_m} \right] \quad (4)$$

244 In Equation 4, X is the water content in dry basis, X_m is the security water
245 content (dry basis), and A is a constant (Caurie, 1981). The security water content
246 presents a commercial viewpoint and it has been related to the maximum water
247 content to prevent an important increase in the rate of deteriorative reactions and
248 assure food stability (Vega-Gálvez et al., 2007). The fitting parameters, calculated by

non-linear regression using the software Microcal Origin v. 6.0 (Microcal Software, Inc., Northampton, USA), resulted in $X_m = 0.0585 \pm 0.0012$ kg water/kg dry matter, $A = 39.1 \pm 3.8$, with a determination coefficient, R^2, of 0.998.

The obtained curve does not show the inflection point that indicates the change between mono- and multi-layer adsorption and this type of isotherm is characteristic of products containing high contents of monosaccharides and sucrose (Tsami, Vagenas & Marinos-Kouris, 1992).

For hot-air dried red bell peppers, Vega-Gálvez et al. (2007) found $X_m = 0.062$ kg water/kg dry matter during adsorption at 20 ^{o}C, whereas Moraes, Rosa and Pinto (2007) found $X_m = 0.064$ kg water/kg dry matter for chitin, following desorption at 20 ºC.

3.2. Glass transition temperatures

Figure 3 shows some of the DSC curves obtained for samples at different water activity. As it was expected in view of the plasticizing effect of water in the hygroscopic region (Slade & Levine, 1991), the glass transition shifted toward lower temperatures with increasing water content. The Gordon and Taylor (1952) model for binary systems (Equation 5) could well represent the glass transition curve in the studied range of a_w (Figure 2). Nevertheless, it should be pointed out that the values of T_g corresponding to the samples of a_w equal to 0.75 and 0.84 were not considered during the fitting procedure. Although these data have shown a good agreement with the glass curve predicted by Equation (5), the obtained thermograms (not shown) presented melting endotherms, indicating the partial crystallization of water during sample cooling.

$$T_g = \frac{X_s T_{gs} + k\, X_w T_{gw}}{X_s + k\, X_w} \quad (5)$$

In Equation (5), X_s is the solids fraction, X_w is the water fraction of the material, T_{gw} is the glass transition of pure amorphous water, considered as -135 ^oC (Slade & Levine, 1991), T_{gs} is the glass transition of the anhydrous solids fraction, and k is an adjustable constant. For grapefruit juice powder, the following values of the fitting parameters were calculated by non-linear regression: $k = 3.92 \pm 0.38$ and $T_{gs} = 44.4 \pm 4.3$ ^oC, with $R^2 = 0.977$. This k value is comparable to those reported for other fruits, such as apple, strawberry, kiwifruit, persimmon, pineapple, and plum (Bai, Rahman, Perera, Smith & Melton, 2001; Moraga, Martinez-Navarrete & Chiralt, 2004, 2006; Sobral, Telis, Habitante & Sereno, 2001; Telis & Sobral, 2001; Telis, Sobral & Telis-Romero, 2006). Roos (1995a) reported values of k of 3.76 for fructose, 4.52 for glucose, and 5.42 for sucrose, reinforcing the hypothesis that T_g of fruits is mainly affected by sugars, present in grapefruit var. Star Ruby juice in a quantity of approximately 0.76 g /g total solids, as discussed in section 2.1. The value obtained for T_{gs} is lower than that presented by Foster et al. (2006) for amorphous sucrose, which is around 57 ºC. This difference can be attributed to the presence of fructose and glucose, as well as citric acid (Shrestha, Ua-Arak, Adhikari, Howes & Bhandari, 2007). According to Roos (1995a), T_g values for anhydrous sucrose, glucose and fructose are, respectively, 62 ºC, 31 ºC and 5 ºC. Considering the proportions of these sugars present in grapefruit (Peiró-Mena, 2007), a weighted average for T_g of the anhydrous mixture would result in 41.2 ºC. The residual moisture content detected at zero water activity must had also affected the experimental value of $T_g = 37.8 \pm 0.3$ ºC measured in the samples of grapefruit juice powder conditioned over P_2O_5.

297 Combining the Caurie and Gordon and Taylor models, it is possible to obtain
298 an equation that relates T_g and a_w (Equation 6), and the curve predicted in this way
299 can be observed in Figure 2. As it can be observed, Equation (6) did not result in a
300 good fitting at water activities near zero. Again, the residual moisture content
301 detected in this sample may be responsible for this lack of agreement.

302 $$T_g = \frac{T_{gs} + kT_{gw}\exp\left[a_w \ln(A) - 1/(4.5X_m)\right]}{1 + k\exp\left[a_w \ln(A) - 1/(4.5X_m)\right]} \quad (6)$$

303 The combination of the water sorption and plasticization behavior of a material
304 would allow the evaluation of food stability, which is lost above T_g (Roos, 1995a,
305 2003). Equation (6) predicts that for grapefruit juice powder stored at $T = T_g = 23\ ^oC$
306 the critical water activity would be 0.118, corresponding to a water content of 0.0346
307 (dry basis). This value of water content is lower than the security water content value
308 calculated using Caurie model. Roos (1987), Moraga et al. (2004, 2006), and Telis et
309 al. (2006) observed the same trend for strawberry, kiwifruit and plum when
310 comparing with the monolayer value obtained from the GAB model, also related to
311 food stability, for sorption isotherms. From this point of view, a_w and T_g must be
312 considered complementary concepts as related to the stability of a product.
313

314 *3.3. Response to compression tests*

315 The mechanical compression tests showed to be adequate to quantify the effect
316 of water uptake on the mechanical properties of the freeze-dried material. Although
317 there was a certain degree of dispersion in the curves of force-displacement and in
318 the value of the maximum force (F_{max}) reached during compression of samples,
319 significant results were obtained by carrying out the assays with at least six replicates
320 at each a_w condition. Since the measurements are simple and fast, the great number

of replicates cannot be considered as a drawback of the method.

Figure 4 shows typical curves of force-displacement obtained for samples equilibrated at different water activities. Except for samples at a_w = 0.75, the force-displacement curves exhibited a continuous and exponential increase in the applied force with distance. A certain degree of stick-slip force fluctuation was observed, which became larger with increasing water activity (see inserts in Figures 4a and 4d). Al Mahdi et al. (2006), during compression of dried skimmed milk, also observed the stick-slip behavior that is revealed by the little up and down fluctuations in the force line. According to these authors, the stick-slip behavior frequently occurs in powder systems. The stick phase corresponds to a gradual accumulation of elastic energy in the powder during compression and is followed by the slip phase in which there is a sudden release of this energy and a decrease in the force. In the freeze-dried grapefruit juice powder, the increasing of stick-slip phenomenon with samples water activity could be associated to a partial and fast relaxation of the applied force, caused by an increase in the plastic behavior of the moist solids.

The maximum force (F_{max}) attained during the compression test showed a strong dependence on the water activity (Figure 5). As it was not possible to use constant sample weights for different water activities because the higher water content juices presented higher densities, F_{max} values were related to sample weight by plotting the ratio F_{max}/m, where m is the sample mass. This ratio was practically constant up to a_w = 0.11 but presented a sudden decrease in the range of $0.11 < a_w < 0.22$. At higher values of a_w, F_{max}/m was essentially constant at a low value. The same behavior was observed when correlating the ratio of compression work (positive area under the compression curve) to the sample mass, as shown in Figure 5. Both parameters revealed the same dependence on sample water activity, showing

346 that the use of different sample mass in the compression tests did not affect the
347 results in a significant magnitude.

348 For $a_w \geq 0.22$ the force-displacement plots exhibited a negative area under the
349 decompression curve (Figures 4b, c, d), which can be related to the sample
350 adhesiveness (Mukherjee & Bhattacharya, 2006; Telis, Telis-Romero & Gabas,
351 2005). Even considering that the compression test applied was not a classical TPA
352 test and that the standard deviations of experimental data were high, the correlation
353 of the decompression works with a_W (insert in Figure 5) shows that the adhesiveness
354 increased with increasing water content, attaining a maximum at $a_w = 0.65$. The trend
355 of decreasing adhesiveness observed at $a_w = 0.75$ could be due to the lubricating
356 effect of water in the samples with higher water content, as it was already pointed out
357 by Mukherjee and Bhattacharya (2006) when studying the compression behavior of
358 rice flour.

359 The Boltzman function, given by Equation (7) and that represents a sigmoid
360 shape curve was fitted to experimental data of F_{max}/m (Figure 5).

361 $$\frac{F_{max}}{m} = \frac{F_u - F_l}{1 + e^{(a_w - a_{whalf})/\lambda}} + F_l \qquad (7)$$

362 In Equation (7), F_u and F_l are the values of F_{max}/m at the upper and lower
363 asymptotes, respectively, λ is a parameter that describes the shape of the curve
364 between the upper and lower asymptotes, and a_{whalf} is the water activity at which
365 F_{max}/m attains the average value between F_u and F_l (White, Silva, Requejo-Tapia &
366 Harker, 2005).

367 The fitting procedure resulted in $F_u = (738 \pm 24) \times 10^3$ N/kg, $F_l = (30 \pm 16) \times$
368 10^3 N/kg, $a_{whalf} = 0.220 \pm 0.001$, with $\lambda = 0.005$. In addition, by differentiating
369 Equation (7), it is possible to determine that the transition between the upper and

lower asymptotes occurs in the range of $0.14 \leq a_w \leq 0.30$. These a_w values correspond to glass transition temperatures of 21.4 ^oC and 6.9 ^oC, respectively, calculated using Equation (6), whereas at $a_{whalf} = 0.22$ the value of T_g is of 14.9 ^oC. Taking into account that the samples storage and measurements were carried out at 23 °C, it is possible to say that the powder susceptibility to stickiness started to increase at $T - T_g \approx 2$ ºC, attained a half intensity at $T - T_g \approx 8$ ºC and was completed at $T - T_g \approx 16$ ºC difference. These magnitudes of temperature differences agree with the results obtained by Foster et al. (2006) when studying the cohesiveness of different freeze-dried sugar powders. These authors showed that, for $T - T_g$ differences of about 10 ºC, development of stickiness was very slow, although powders left for a long time at this condition could develop significant levels of cohesiveness. On the other hand, for $T - T_g$ in the range of 19 to 41 ºC instantaneous occurrence of stickiness could be observed in the various sugars. Using thermal mechanical analysis, Venir et al. (2007) measured the collapse temperature of freeze-dried apple tissue and found a constant difference of 10 ºC higher than T_g up to $a_w = 0.5$. At higher a_w values this difference increased, which was attributed to the changes of material properties at the onset of shrinkage.

3.4. Color development

The analysis of color carried out after compression of samples proved satisfactory in order to obtain reproducible results. The compression contributed to reduce the influence of sample porosity and non-uniform surface on color measurements, as well as generated samples of similar thickness (2.53 ± 0.23 mm), a characteristic that would be difficult to obtain after the conditioning at different relative humidity due to collapse occurrence.

395 The measured color coordinates L*, a*, and b* of six replicates showed small
396 standard deviations throughout the range of studied a_w, as shown in Figure 6. Their
397 values remained practically constant up to a_w = 0.43 and then showed a continuous
398 decrease, mainly in the lightness, because of browning development. The total color
399 difference, ΔE*, calculated with reference to the powder conditioned over P_2O_5
400 (Figure 7) clearly showed that a water activity of 0.43 was a critical value that
401 limited two distinct a_w domains. Below this value, there was a slight change in
402 sample color with increasing a_w. This change seems to be a result of a slight increase
403 in a* and b* and a reduction of L* (Figure 6). Above a_w = 0.43, the effect of
404 increasing water activity was much more pronounced. In the domain of higher water
405 activities, it was possible to observe a great reduction in the chroma and lightness of
406 the juice with increasing a_w, although the hue angle did not show a clear tendency.
407 Venir et al. (2007) and Acevedo et al. (2006) observed negligible color changes
408 in freeze-dried apple tissue at low a_w and maximum browning at a_w = 0.50, whereas
409 more hydrated samples exhibited reduced browning. This behavior was attributed to
410 the optimal conditions of diffusion and concentration of oxidized phenols for
411 browning at intermediate a_w and to the dilution of reactants at higher a_w that could
412 account for a lower browning. Acevedo, Schebor and Buera (2008) have also
413 reported the occurrence of a maximum in the rate of non-enzymatic browning in
414 freeze-dried potato discs conditioned at a_w = 0.84 and a decrease in this rate at high
415 water activities (a_w = 0.93). In the present work, there was no evidence of a
416 maximum in the curve of ΔE* up to a_w = 0.75, although measurements at higher
417 water activities would be necessary to clarify the behavior at higher a_w conditions.
418 The analysis of the total color differences in terms of $T - T_g$ indicated that the
419 critical temperature difference for browning of samples was around 32 ºC, which

configures a higher temperature departure from T_g than the observed critical temperature difference for mechanical changes occurrence. This behavior suggests that from the perspective of the time at which mechanical and color changes would take place, the stickiness development in the grapefruit juice powder would precede browning.

4. Conclusion

Confined compression tests gave reproducible and significant results in terms of the maximum force attained during compression (F_{max}) of samples at different a_w and showed to be adequate as indicative of mechanical changes that may be related to stickiness development in the freeze-dried powdered juice, as well as contributed to generate samples with uniform surface for color evaluation. Mechanical and color changes were related to glass transition temperature and to water activity. The appearance of changes in mechanical properties showed to precede significant color changes when taking into account a scale of increasing water activity: a free flowing powder of grapefruit juice was only obtained at very low water activity ($a_w \leq 0.14$, $T - T_g \approx 2$ ºC), whereas intense color changes were observed only at higher water activities ($a_w \geq 0.43$, $T - T_g \approx 32$ ºC).

5. Acknowledgement

Authors thank the Ministerio de Educación y Ciencia and the Fondo Europeo de Desarrollo Regional (FEDER) for the financial support throughout the projects AGL2002-01793 and AGL 2005-05994. Vânia R. N. Telis acknowledges the support of the Coordenação de Aperfeiçoamento de Pessoal de Nível Superior (CAPES) as an external grant (Proc. BEX 4452/06-2).

6. References

Acevedo, N., Schebor, C., & Buera, M. P. (2006). Water–solids interactions, matrix structural properties and the rate of non-enzymatic browning. *Journal of Food Engineering*, 77, 1108-1115.

Acevedo, N., Schebor, C., & Buera, M. P. (2008). Non-enzymatic browning kinetics analysed through water–solids interactions and water mobility in dehydrated potato. *Food Chemistry*, 108, 900-906.

Adhikari, B., Howes, T., Bhandari, B. R., & Troung, V. (2004). Effect of addition of maltodextrin on drying kinetics and stickiness of sugar and acid-rich foods during convective drying experiments and modelling. *Journal of Food Engineering*, 62, 53-68.

Aguilera, J. M., Del Valle, J. M., & Karel, M. (1995). Caking phenomena in amorphous food powders. *Trends in Food Science & Technology*, 6, 149-155.

Al Mahdi, R., Nasirpour, A., Banon, S., Scher, J., & Desobry, S. (2006). Morphological and mechanical properties of dried skimmed milk and wheat flour mixtures during storage. *Powder Technology*, 163, 145-151.

Bai Y., Rahman M. S., Perera C. O., Smith B. & Melton L. D. (2001). State diagram of apple slices: glass transition and freezing curves. *Food Research International*, 34, 89-95.

Bonelli, P., Schebor, C., Cukierman, A. L., Buera, M. P., & Chirife, J. (1997). Residual water content as related to collapse of freeze-dried sugar matrices. *Journal of Food Science*, 62(4), 693-695.

Boonyai, P., Bhandari, B., & Howes, T. (2004). Stickiness measurement techniques: a review. *Powder Technology*, 145(1), 34-46.

Boonyai, P., Howes, T., & Bhandari, B. (2007). Instrumentation and testing of a thermal mechanical compression test for glass–rubber transition analysis of food powders. *Journal of Food Engineering*, 78, 1333–1342.

Brooks, G. F., Paterson A. H. J., & Bronlund, J. E. (2001). Residual moisture in amorphous lactose and its effect on Tg. Conference of food engineering, AICHE conference (pp. 401–407). Reno, Nevada, USA. 4–9 November 2001.

Caurie, M. (1970). A new model equation for predicting safe storage moisture levels for optimum stability of dehydrated foods. *Journal of Food Technology*, 5, 301–307.

Caurie, M. (1981). Derivation of full range moisture sorption isotherms. In L. B. Rockland, & G. F. Stewart. Water activity: influences on food quality (pp. 63-87). New York: Academic Press.

Chen, X. D. (2007). Conformability of the kinetics of cohesion/stickiness development in amorphous sugar particles to the classical Arrhenius law. *Journal of Food Engineering*, 79, 675–680.

Fernandez-Segovia, I., Camacho, M. M., Martinez-Navarrete, N., Escriche, I., & Chiralt A. (2003). Structure and color changes due to thermal treatments in desalted cod. *Journal of Food Processing and Preservation*, 27, 465-474.

Fitzpatrick, J. J., Hodnett, M., Twomey, M., Cerqueira, P. S. M., O'Flynn, J., & Roos, Y. H., (2007). Glass transition and the flowability and caking of powders containing amorphous lactose. *Powder Technology*, 178, 119-128.

Foster, K. D., Bronlund, J. E., & Paterson A. H. J. (2006). Glass transition related cohesion of amorphous sugar powders. *Journal of Food Engineering*, 77, 997-1006.

Gordon, M., & Taylor, J. S. (1952). Ideal copolymers and the second order

transitions of synthetic rubbers. I. Non-crystalline copolymers. *Journal of Applied Chemistry*, 2, 493-500.

Karel, M. (1973). Recent research and development in the field of low moisture and intermediate-moisture foods. *CRC Critical Review Food Technology*, 3, 329-373.

Karmas, R., Buera M. P., & Karel, M. (1992). Effect of glass transition on rates of nonenzymatic browning in food systems. *Journal of Agricultural and Food Chemistry*, 40, 873-879.

Konica Minolta Sensing, Inc. (2003). Precise color communication. Color control from perception to instrumentation. 59 p. Access in May 06, 2008. http://www.konicaminolta.com/instruments/knowledge/color/index.html

Krokida, M. K., Maroulis, Z. B., & Saravacos, G. D. (2001). The effect of the method of drying on the colour of dehydrated products. *International Journal of Food Science and Technology*, 36, 53-59.

Labuza, T. P. (1980). The effect of water activity on reaction kinetics of food deterioration. *Food Technology*, 34(4), 36-41, 59.

Levi, G., & Karel, M. (1995). Volumetric shrinkage (collapse) in freeze-dried carbohydrates above their glass transition temperature. *Food Research International*, 28(2), 145-151.

Levine, H., & Slade, L. (1989). A food polymer science approach to the practice of cryostabilization technology. *Comments on Agriculture and Food Chemistry*, 1(6), 315-396.

Lievonen, S. M., Laaksonen, T. J., & Roos Y. H. (2002). Nonenzymatic browning in food models in the vicinity of the glass transition: effects of fructose, glucose, and xylose as reducing sugar. *Journal of Agricultural and Food Chemistry*, 50,

7034-7041.

Ling, H. -I., Birch, J., & Lim, M. (2005). The glass transition approach to determination of drying protocols for colour stability in dehydrated pear slices. *International Journal of Food Science and Technology*, 40, 921-927.

Miao, S., & Roos, Y. H. (2006). Isothermal study of nonenzymatic browning kinetics in spray-dried and freeze-dried systems at different relative vapor pressure environments. *Innovative Food Science and Emerging Technologies*, 7, 182-194.

Moraes, M. A., Rosa, G. S., & Pinto, L. A. A. (2007). Isotermas de equilíbrio para quitina: determinação do calor de dessorção. *Brazilian Journal of Food Science and Technology*, 10(3), 212-219.

Moraga, G., Martínez-Navarrete, N., & Chiralt, A. (2004). Water sorption isotherms and glass transition in strawberries: influence of pretreatment. *Journal of Food Engineering*, 62, 315-321.

Moraga, G., Martinez-Navarrete, N., & Chiralt, A. (2006). Compositional changes of strawberry due to dehydration, cold storage and freezing-thawing processes. *Journal of Food Processing and Preservation*, 30(4), 458-474.

Mukherjee, C., & Bhattacharya, C. (2006). Characterization of agglomeration process as a function of moisture content using a model food powder. *Journal of Texture Studies*, 37, 35-48.

Özkan, N., Walisinghe, N., & Chen, X. D. (2002). Characterization of stickiness and cake formation in whole and skim milk powders. *Journal of Food Engineering*, 55, 293-303.

Paterson, A. H. J., Brooks, G. F., Bronlund, J. E., & Foster, K. D. (2005). Development of stickiness in amorphous lactose at constant T - T_g levels.

International Dairy Journal, 15, 513-519.

Peiró-Mena, R. (2007). Cambios en los micronutrientes y compuestos fitoquímicos asociados al procesado osmótico de frutas y su estabilidad en un producto gelificado. Ph.D. thesis, Polytechnic University, Valencia, Spain.

Phanindrakumar, H. S., Radhakrishna, K., Mahesh, S., Jagannath, J. H., & Bawa, A. S. (2005). Effect of pretreatments and additives on the thermal behavior and hygroscopicity of freeze-dried pineapple juice powder. *Journal of Food Processing and Preservation*, 29, 307-318.

Prado S. M., Buera M. P., & Elizalde B. E. (2006). Structural collapse prevents β-carotene loss in a supercooled polymeric matrix. *Journal of Agricultural and Food Chemistry*, 54, 79-85.

Rampersaud, G. C. (2007). A comparison of nutrient density scores for 100% fruit juices. *Journal of Food Science*, 72(4)**,** S261-S266.

Roos, Y., & Karel, M. (1991). Applying state diagrams to food processing and development. *Food Technology*, 45(12), 66-71.

Roos, Y. H. (1987). Effect of moisture on the thermal behavior of strawberries studied using differential scanning calorimetry. *Journal of Food Science*, 52, 146-149.

Roos, Y. H. (1995a). Characterization of food polymers using state diagrams. *Journal of Food Engineering*, 24(3), 339-360.

Roos, Y. H. (1995b). Phase transitions in foods. San Diego: Academic Press.

Roos, Y. H. (2003). Thermal analysis, state transitions and food quality. *Journal of Thermal Analysis and Calorimetry*, 71, 197-203.

Shrestha, A. K., Ua-Arak, T., Adhikari, B. P., Howes, T., & Bhandari, B. R. (2007). Glass transition behavior of spray dried orange juice powder measured by

differential scanning calorimetry (DSC) and thermal mechanical compression test (TMCT). *International Journal of Food Properties*, 10(3), 661-673.

Slade, L., & Levine, H. (1991). Beyond water activity: recent advances based on an alternative approach to the assessment of food quality and safety. *Critical Reviews on Food Science and Nutrition*, 30, 115-360.

Sobral, P. J. A., Telis, V. R. N., Habitante, A. M. Q. B. & Sereno, A. (2001). Phase diagram for freeze-dried persimmon. *Thermochimica Acta*, 376, 83-89.

Spiess, W. E. L., & Wolf, W. R. (1983). The results of the COST 90 project on water activity. In F. Escher, B. Hallstrom, H.S. Meffert, W.E.L. Spiess, & G. Voss (Eds.), *Physical Properties of Foods* (pp. 65-87). Applied Science Publishers, New York.

Telis, V. R. N., & Sobral, P. J. A. (2001). Glass transitions and state diagram for freeze-dried pineapple. *Lebensmittel-Wissenschaft und-Technologie*, 34(4), 199-205.

Telis, V. R. N., Sobral, P. J. A., Telis-Romero, J. (2006). Sorption isotherm, glass transitions and state diagram for freeze-dried plum skin and pulp. *Food Science and Technology International*, 12(3), 181-187.

Telis, V. R. N., Telis-Romero, J., & Gabas, A. L. (2005). Solids rheology for dehydrated food and biological materials. *Drying Technology*, 23(4), 759-780.

To, E. C., & Flink, J. M. (1978). Collapse, a structural transition in freeze dried carbohydrates I. Evaluation of analytical methods. *Jounal of Food Technology*, 13, 551-565.

Tsami, E., Vagenas, G. K., & Marinos-Kouris, D. (1992). Moisture sorption isotherms of pectins. *Journal of Food Processing and Preservation*, 16(3), 151-161.

595 Vega-Gálvez, A., Lemus-Mondaca, R., Fito, P., & Andrés, A. (2007). Note: moisture
596 sorption isotherms and isosteric heat of red bell pepper (var. Lamuyo). *Food*
597 *Science and Technology International*, 13(4), 309-316.
598 Venir, E., Munari, M., Tonizzo, A., & Maltini, E. (2007). Structure related changes
599 during moistening of freeze dried apple tissue. *Journal of Food Engineering*,
600 81, 27-32.
601 White, K. L., & Bell, L. N. (1999). Glucose loss and Maillard browning in solids as
602 affected by porosity and collapse. *Journal of Food Science*, 64(6), 1010-1014.
603 White, A., Silva, H. N., Requejo-Tapia, C., Harker, F. R. (2005). Evaluation of
604 softening characteristics of fruit from 14 species of *Actinidia*. *Postharvest*
605 *Biology and Technology*, 35, 143–151.
606

607 **Figure Captions**

608 Figure 1. Schematic diagram of the sample holder used for the compression tests

609

610 Figure 2. Sorption isotherm at 23 ^{o}C and glass transition temperatures for freeze-
611 dried grapefruit juice powder: (■) water content (dry basis); (——) Caurie model
612 (Equation 4); (○) T_g (^{o}C); (– – – –) Equation 6

613

614 Figure 3. Typical DSC curves obtained for freeze-dried grapefruit juice powder at
615 different a_w.

616

617 Figure 4. Typical curves of force-displacement obtained during mechanical
618 compression tests of freeze-dried grapefruit juice powder at different a_w and 23 ^{o}C:
619 (a) a_w = 0; (b) a_w = 0.22; (c) a_w = 0.53; (d) a_w = 0.75. The inserts in (a) and (d) are
620 magnified curves to show the stick-slip behavior

621

622 Figure 5 Mechanical properties for freeze-dried grapefruit juice powder as function
623 of a_w at 23 ^{o}C: (■) F_{max} per unit of mass sample; (○) compression work per unit of
624 mass sample; (——) Equation (7). The insert shows the adhesiveness of the samples
625 at different a_w. Mean values and standard deviation of six replicates

626

627 Figure 6. CIELab color coordinates for freeze-dried grapefruit juice powder as
628 function of a_w: (▼) L*; (Δ) a*; (•) b*. Mean values and standard deviation of six
629 replicates

630

631 Figure 7. Color attributes for freeze-dried grapefruit juice powder as function of a_w:

632 (▼) hue angle, h_{ab}*; (Δ) chroma, C_{ab}*; (•) total color differences, ΔE*

Figure 1

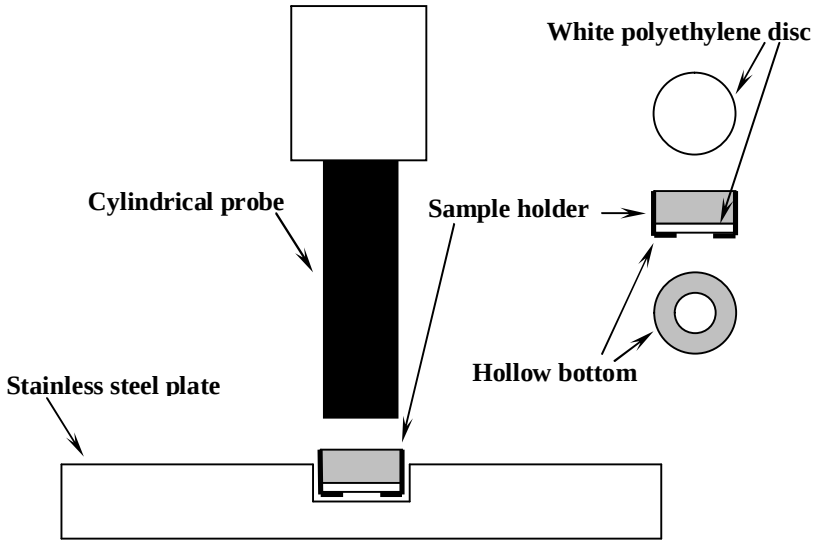
White polyethylene disc
Cylindrical probe
Sample holder
Hollow bottom
Stainless steel plate

Figure 2

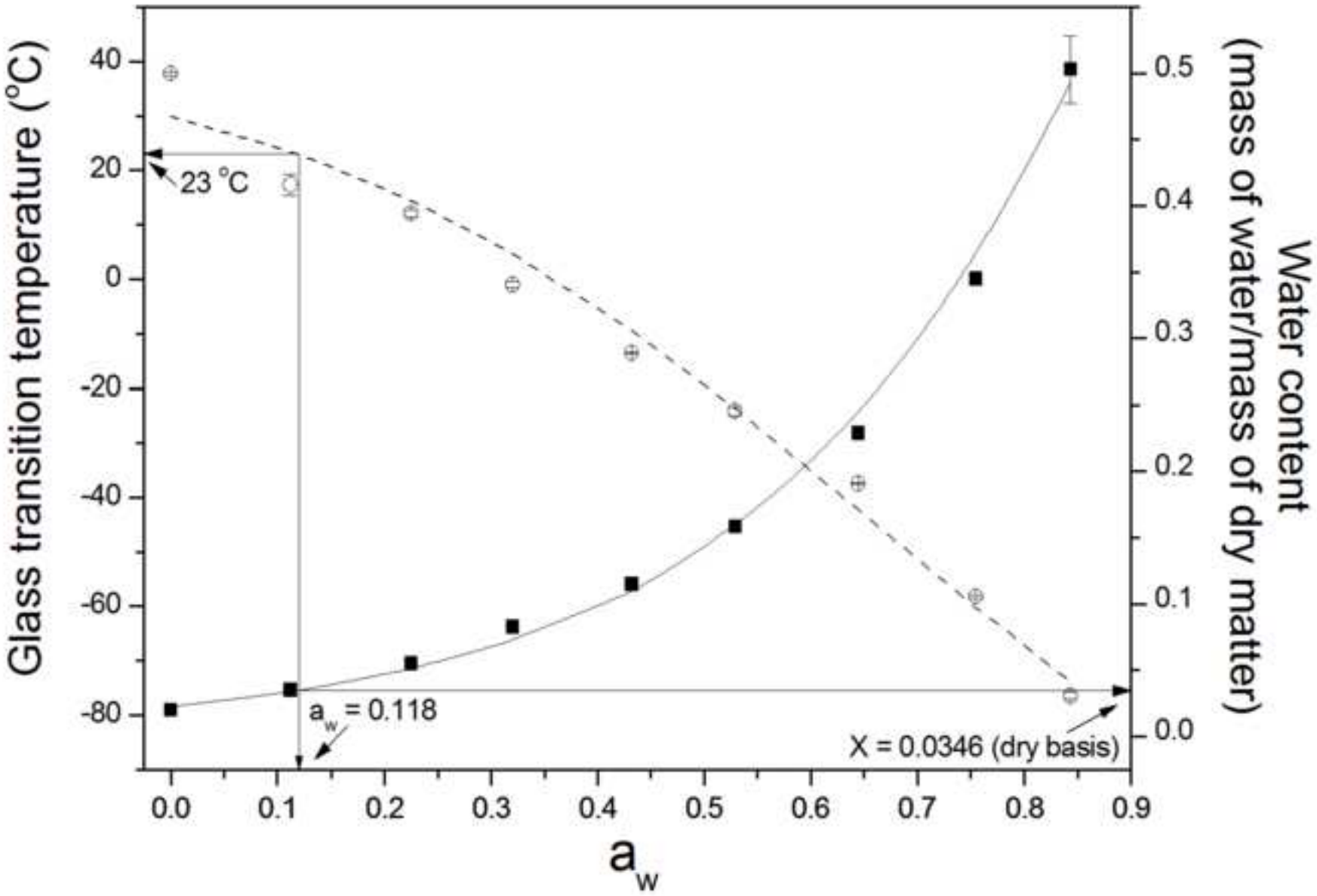
Glass transition temperature (°C)
Water content
(mass of water/mass of dry matter)
a_w
23 °C
a_w = 0.118
X = 0.0346 (dry basis)
40
20
0
-20
-40
-60
-80
0.5
0.4
0.3
0.2
0.1
0.0
0.0
0.1
0.2
0.3
0.4
0.5
0.6
0.7
0.8
0.9

Figure 3

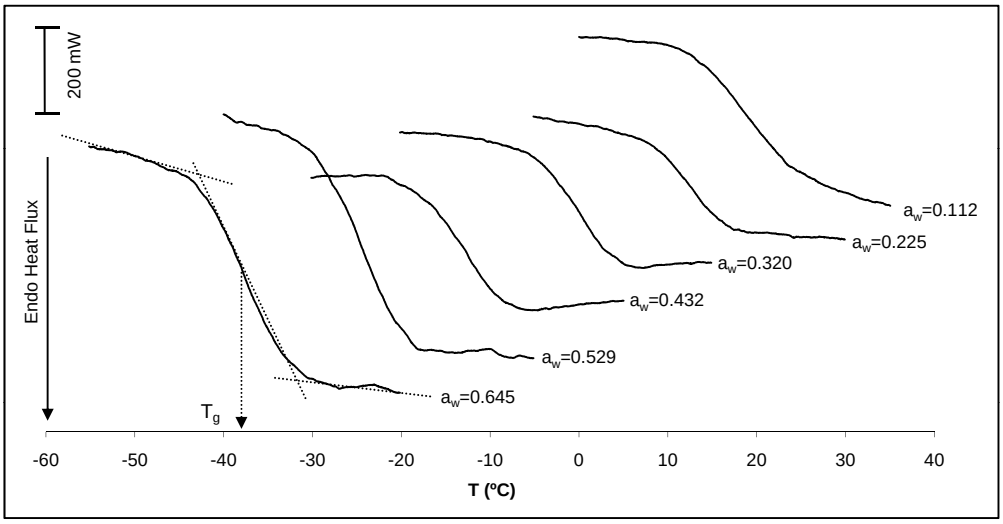
200 mW
Endo Heat Flux
a_w=0.112
a_w=0.225
a_w=0.320
a_w=0.432
a_w=0.529
a_w=0.645
T_g
-60
-50
-40
-30
-20
-10
0
10
20
30
40
T (ºC)

Figure 4

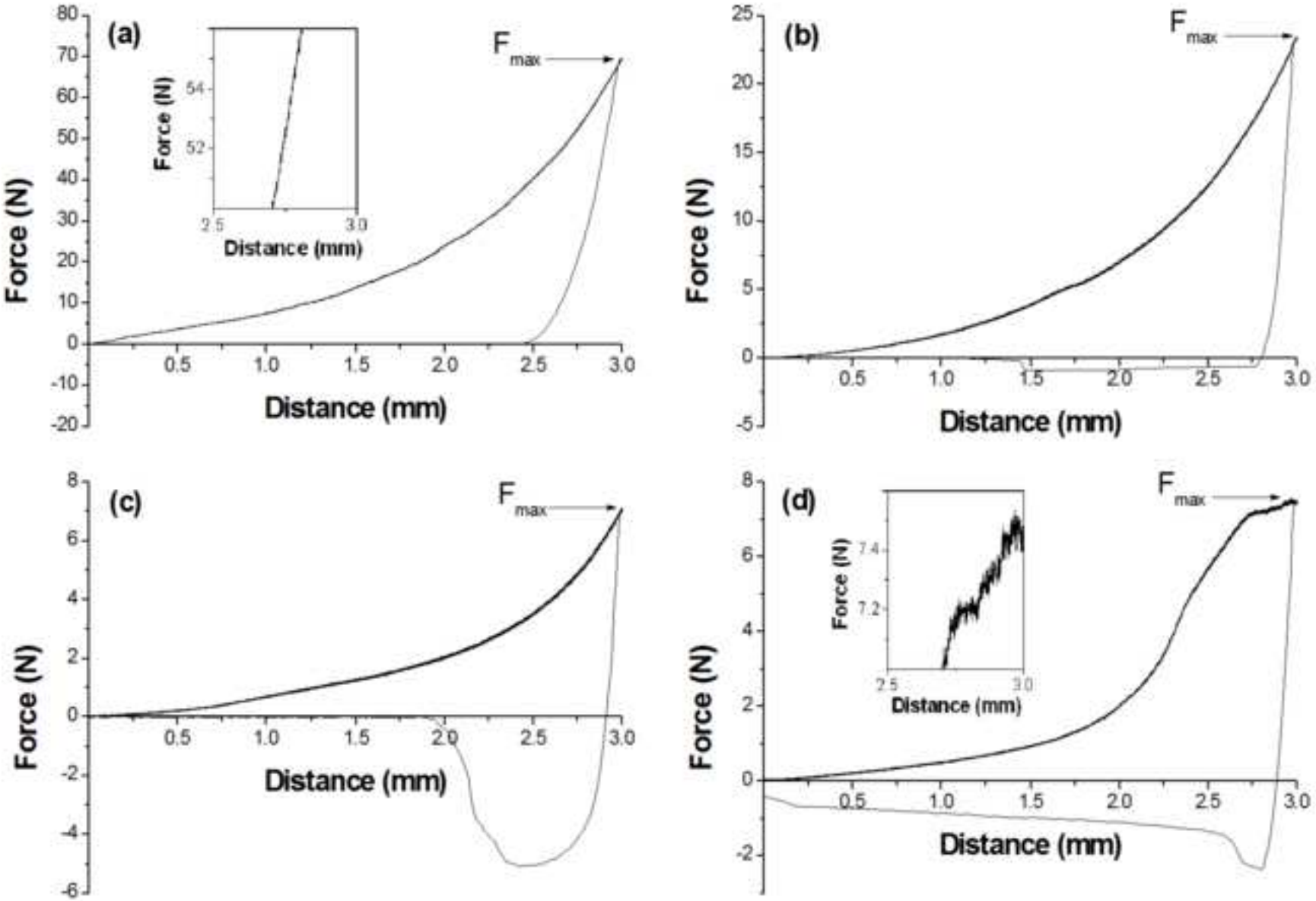
(a)
Force (N)
Distance (mm)
F max
(b)
Force (N)
Distance (mm)
F max
(c)
Force (N)
Distance (mm)
F max
(d)
Force (N)
Distance (mm)
F max

Figure 5

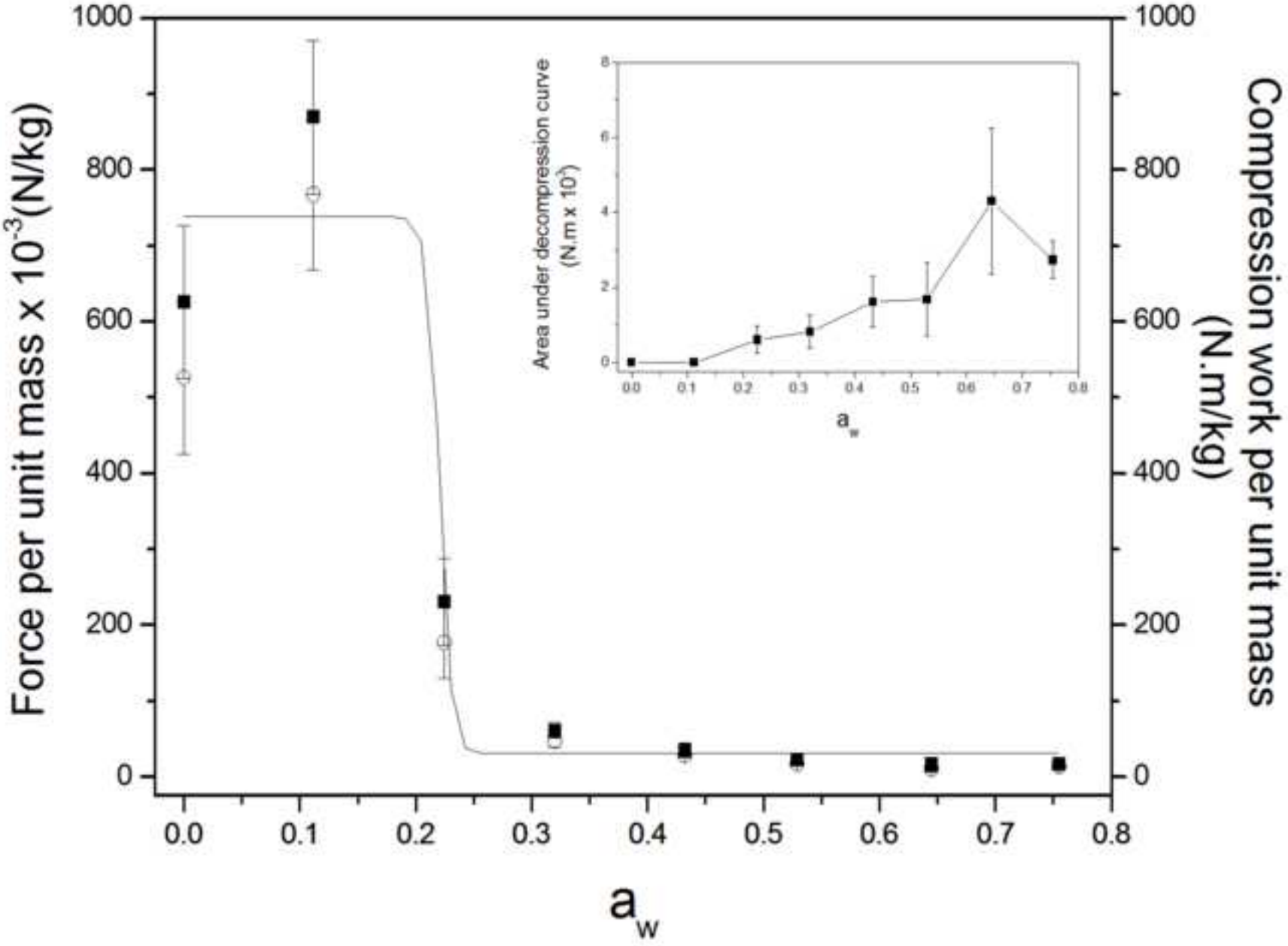
Force per unit mass x 10-3(N/kg)
Compression work per unit mass (N.m/kg)
aw
Area under decompression curve (N.m x 10-3)
aw
0
200
400
600
800
1000
0.0
0.1
0.2
0.3
0.4
0.5
0.6
0.7
0.8

Figure 6

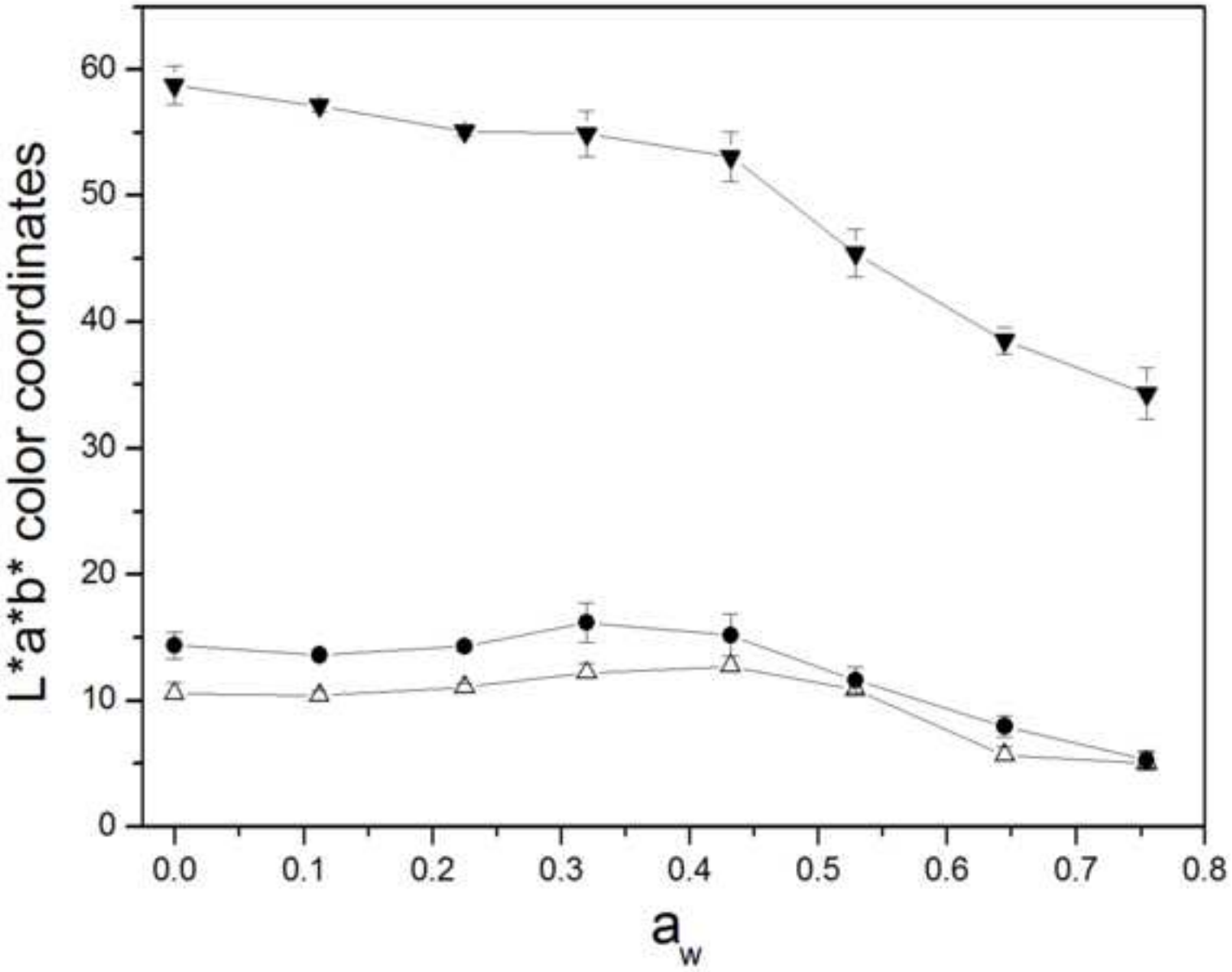
L*a*b* color coordinates
60
50
40
30
20
10
0
0.0
0.1
0.2
0.3
0.4
0.5
0.6
0.7
0.8
a_w

Figure 7

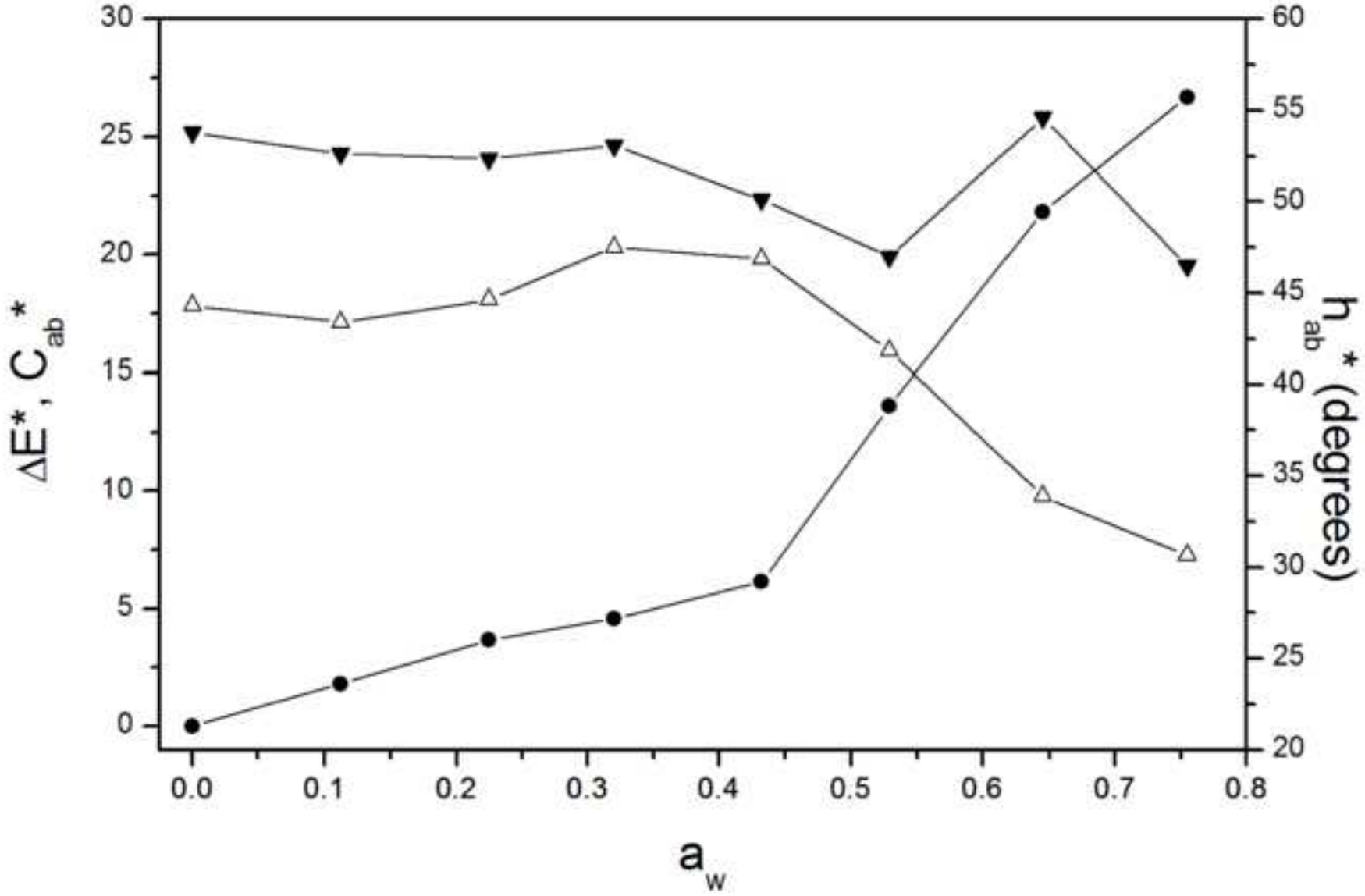
30
25
20
15
10
5
0
60
55
50
45
40
35
30
25
20
0.0
0.1
0.2
0.3
0.4
0.5
0.6
0.7
0.8
ΔE*, C*ab
h*ab (degrees)
aw